Efficient trajectory parameterization for environmental optimization of departure flight paths using a genetic algorithm

Hartjes, Sander; Visser, H.G.

Important note
To cite this publication, please use the final published version (if applicable).
Please check the document version above.

Efficient trajectory parameterization for environmental optimization of departure flight paths using a genetic algorithm

S Hartjes and HG Visser

Abstract
In this study, a genetic optimization algorithm is applied to the design of environmentally friendly aircraft departure trajectories. The environmental optimization has been primarily focused on noise abatement and local NO_x emissions, whilst taking fuel burn into account as an economical criterion. In support of this study, a novel parameterization approach has been conceived for discretizing the lateral and vertical flight profiles, which reduces the need to include nonlinear side constraints in the multiparameter optimization problem formulation, while still permitting to comply with the complex set of operational requirements pertaining to departure procedures. The resulting formulation avoids infeasible solutions and hence significantly reduces the number of model evaluations required in the genetic optimization process. The efficiency of the developed approach is demonstrated in a case study involving the design of a noise abatement departure procedure at Amsterdam Airport Schiphol in The Netherlands.

Introduction

Due to the continuing growth in air traffic demand and the rising level of urbanization around many airports, aviation is having an ever greater impact on the human environment. Spurred by a growing public awareness on environmental issues, this greater impact leads to a larger demand for accountability towards airlines, airports and governments, and hence to an increase in technical or regulatory measures to reduce the environmental burden.[1] In addition to the noise nuisance caused by aviation, the local environmental impact of gaseous emissions is receiving increasingly more attention.[1] In response to the need to improve the environmental footprint of flight operations, considerable research is currently being conducted towards the development of environmentally friendly flight paths.[1]

Research in the field of environmentally optimized trajectories has indeed been quite extensive in recent years. Prats et al.[2] applied numerical optimization techniques in an effort to minimize the noise impact in a number of discrete highly noise-sensitive areas. Focusing directly on community noise impact, Hartjes et al.[3] explored noise-optimized departures using gradient-based optimization techniques, whilst Hogenhuis et al.[4] conducted a similar study pertaining to arrivals. The study of Fernandes de Oliveira and

Büskens[5] focused on flight profile optimization along recorded ADS-B ground tracks for flights departing from Frankfurt airport. Richter et al.[6] developed a noncooperative bi-level optimal control problem formulation for noise-minimal departure trajectories. In this study, noise was optimized at the upper level problem, whilst direct operational cost minimization was considered at the lower level. Torres et al.[7] used a multi-objective mesh adaptive direct search (multi-MADS) method to optimize departure trajectories for NOx emissions and noise at a single measurement point, without requiring gradient information.

Previous research has mostly focused on single-objective optimization, using gradient-based optimization techniques. Although very efficient in finding optimal trajectories, these techniques require the definition of a single optimization criterion (which can be a composite of different objectives), and generate a single optimal trajectory. Moreover, gradient-based methods can only be applied in conjunction with

Faculty of Aerospace Engineering, Delft University of Technology, Delft, The Netherlands

Corresponding author:
HG Visser, Faculty of Aerospace Engineering, Delft University of Technology, P.O. Box 5058, 2600 GB Delft, The Netherlands.
Email: h.g.visser@tudelft.nl

models that are expressed in terms of smooth differentiable functions. Therefore, in this study, a multi-objective (gradient-free) genetic optimization algorithm has been employed to find a set of solutions for a range of optimization criteria, focusing on fuel burn, NOx emissions, and community noise impact.

However, genetic algorithms generally require large numbers of problem evaluations, and hence extensive runtimes in order to find optimal trajectories. To reduce the required number of function evaluations, a novel parameterization technique is proposed in this study for both the lateral and vertical trajectory, which aims to reduce the need to explicitly include algebraic side constraints in the optimization formulation, and at the same time precludes the generation of infeasible solutions. As a result, each trajectory generated is flyable and complies with the boundary conditions and most of the operational constraints imposed on the problem.

To illustrate the capabilities of the proposed methodology, a Standard Instrument Departure (SID) currently in use at Amsterdam Airport Schiphol (AMS) has been parameterized and optimized with respect to community noise impact, fuel burn, and local NOx emissions using a Boeing 737-800 aircraft model. The presented study has been carried out in the framework of the Systems for Green Operations (SGO) Industrial Technology Demonstrator (ITD), part of the CleanSky Joint Technology Initiative (JTI) of the European Union.[8]

The structure of this article is as follows. First, the optimization method employed is described, followed by an overview of the aircraft model and the noise and emission models used. Next, the parameterization is explained, followed by an example scenario and its results. Finally, the conclusions and recommendations for future work are stated.

Optimization framework

As part of the CleanSky SGO ITD, this study relies on the Green Aircraft Trajectories under ATC Constraints (GATAC) optimization framework.[9] The GATAC framework offers a graphic user interface (GUI) for the trajectory optimization problem setup and allows for an easy integration of different model types required to run the problem. In addition, GATAC offers the use of multiple optimization methodologies to find optimal aircraft trajectories. For this study, a customized genetic algorithm is used based on the non-dominated sorting algorithm (NSGA-II).[10] The set of final nondominated solutions is referred to as the Pareto-optimal front. The algorithm used in this study, called NSGAMO-2, differs from NSGA-II primarily in the selection process of the mating pool, and the genetic operators.[11]

To conduct this study, three different models were implemented in the GATAC framework, namely an aircraft performance model including engine, fuel flow and gaseous emissions models, an aircraft noise model, and a community noise impact model.

Aircraft performance modeling

The aircraft model used in this study is a so-called intermediate point-mass model.[3,4] This system model is somewhat simplified in the sense that equilibrium of forces normal to the flight path is assumed. The implication of this simplifying assumption is that the aerodynamic drag is slightly underestimated since it is evaluated as if the aircraft performs a quasi-linear flight. Further assumptions made in the model formulation include: (1) no wind present, (2) the Earth is flat and nonrotating, and (3) the flight is coordinated (no sideslip). In addition, the flight path angle is considered small ($\gamma < 15°$) and during the departure procedure the aircraft weight W is considered constant. With these assumptions, the equations of motion can be written as

$$
\begin{aligned}
\dot{x} &= V \cos \gamma \sin \chi \\
\dot{y} &= V \cos \gamma \cos \chi \\
\dot{h} &= V \sin \gamma \\
\dot{\chi} &= \frac{g \tan \mu}{V} \\
\dot{V} &= g \left(\frac{(T - D)}{W} - \sin \gamma \right)
\end{aligned}
\tag{1}
$$

Note that in equation (1), $x(t)$, $y(t)$, $h(t)$ are the state variables representing the location of the aircraft in the three-dimensional space, $\chi(t)$ is the heading angle of the aircraft, and $V(t)$ is the true airspeed. In this equation, D represents the aerodynamic drag. Assuming a parabolic drag polar, the drag force D in the intermediate model can be expressed as

$$
D = C_{D_0} \frac{1}{2} \rho V^2 S + \frac{K(\tan^2 \mu + 1) W^2}{\frac{1}{2} \rho V^2 S} = D(h, V, \mu, W)
\tag{2}
$$

where C_{D_0} and K are the drag polar parameters, ρ is the air density, and S is the aircraft wing surface area.

The control variables governing the point-mass system equations (1) are flight path angle $\gamma(t)$, bank angle $\mu(t)$, and thrust $T(t)$. Using parameterized control functions as inputs, the differential equations defining the system dynamics can be propagated forward in time, from a given initial state. In this study, a fourth-order Runge–Kutta integration scheme with a fixed 0.1 second time-step has been employed for this purpose.

To be able to assess airline commercial interests in the form of fuel burn, an additional state variable has been added to the model which indicates the cumulative fuel consumption along the trajectory. Furthermore, the total amount of NOx emitted has

also been added as a state variable. The corresponding state equation is given by

$$\dot{m}_{NO_x} = \dot{m}_f EI_{NO_x} \qquad (3)$$

where m_{NO_x} is the mass of the emitted NO_x, $\dot{m}_f$ is the fuel flow rate, and EI_{NO_x} is the emission index for NO_x in g/kg of burned fuel burned. The emission index is extracted from the ICAO Engine Emission Databank.[12] This databank contains certification data on a number of gaseous emissions for most modern jet engines, measured under reference conditions for four typical thrust settings. To account for off-reference atmospheric conditions and thrust levels, the ICAO data needs to be corrected. For this purpose, the emissions model is augmented with the Boeing Method 2 (BM2).[13] The Boeing Method 2 provides a means for interpolating the ICAO emissions data, and applies a number of corrections for atmospheric conditions and airspeed effects. The resulting corrected emissions index for NO_x is used in this study to determine the total amount of NO_x emitted. Further details regarding the employed fuel and emissions model can be found in Hartjes et al.[3]

Aside from the total fuel burn and noise impact, the amount of local NO_x emissions is adopted as an optimization criterion in this study. Local emissions are emissions that have a direct impact on the human environment, and are defined as emitted below 3000 ft above ground level (AGL).

Noise and noise impact modeling

The acoustic model integrated in the optimization setup in this study is based on the widely used integrated noise model (INM), version 7.0b.[14] The noise model used in this study is a replication of the in-flight noise assessment model incorporated in INM. The model can provide a number of noise metrics for the majority of modern commercial aircraft, and is based on empirically determined noise–power–distance tables. These tables are interpolated for the thrust level and the distance between the observer and the flight segment and are based on the assumption that the observer is standing directly below an aircraft passing along a straight segment of infinite length at a given reference speed. To correct for nonreference conditions, a number of adjustments are introduced. To assess the community noise impact of individual departing aircraft, the population density distribution in the vicinity of the aircraft is required. In addition, the community noise impact needs to be quantified. To accommodate these requirements, this study uses a geographic information system (GIS) containing population density information, and a dose–response relationship to quantify the noise impact. The dose–response relationship used in this study is based on research done by the Federal Interagency Committee on Aviation Noise (FICAN) in 1997 and yields an upper limit to the percentage of expected awakenings due to a single nighttime flyover.[15] This percentage can be expressed as (see Figure 1)

$$\%Awakenings = .0087\,(SEL_{indoor} - 30\,)^{1.79} \qquad (4)$$

where SEL_{indoor} is the indoor sound exposure level.

As the noise model calculates the outdoor SEL, a 20.5 dB correction is applied to account for the sound absorption of an average house.[1] By calculating the SEL on each of the grid points in the GIS in which
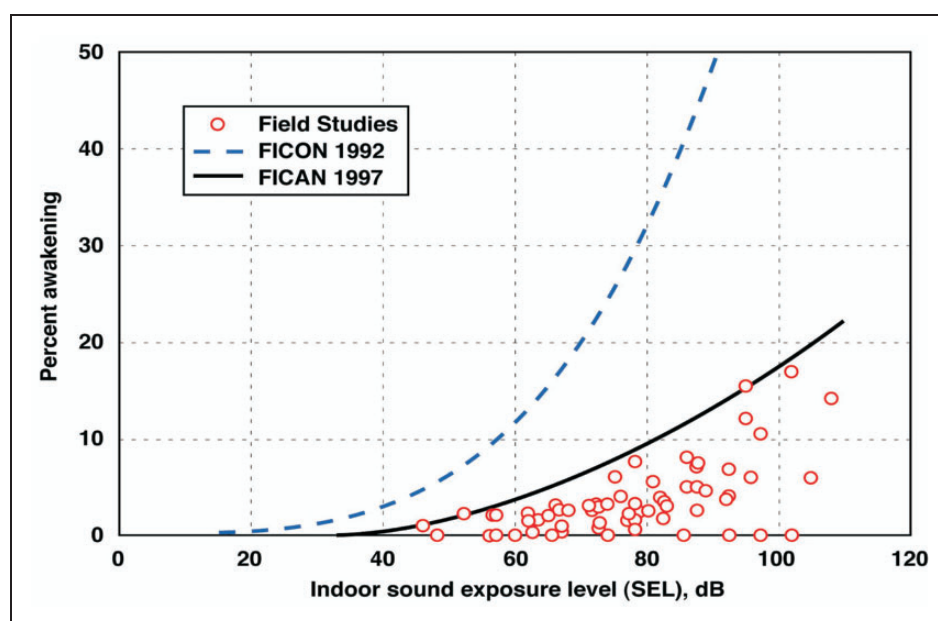

Figure 1. FICAN dose–response relationship.
FICAN: Federal Interagency Committee on Aviation Noise.

population is present, and multiplying the number of people living in a particular grid point with the expected percentage of awakenings, the total maximum number of expected awakenings can be determined. This metric then serves as the noise criterion in the trajectory optimization problem definition.

Trajectory parameterization

Although genetic optimization algorithms are very robust in nature, one of the main issues in applying them concerns the number of model evaluations required to find the Pareto-optimal set of solutions. The required runtime to achieve acceptable convergence conditions is usually considerable, especially when a large number of control parameters are considered. Imposing (equality or inequality) side constraints in the optimization formulation through the inclusion of penalties or barriers will further adversely affect the convergence behavior, as more model evaluations are required. In this study, a novel parameterization approach has been used that permits a relatively large number of optimization parameters, and minimizes the required number of constraints to be included in the problem formulation, whilst still optimizing a three-dimensional trajectory that satisfies all operational requirements. In the proposed parameterization approach, the first step is to separately parameterize the vertical (procedure) and lateral (routing) parts of the trajectory.

Lateral track parameterization

In this study, the synthesis of departure routes has been based on the usage of a modern navigation technology known as required navigation performance (RNP). An RNP route can be loosely defined as a sequence of lateral directives along a set of waypoints, enabling to construct a flight path between waypoints

that can be pre-programmed and automatically executed using the flight management system (FMS) technology currently available in most aircraft. In order to be able to avoid noise-sensitive areas, and to minimize flight track dispersion, the use of RNP and more specifically track-to-a-fix (TF) legs and radius-to-a-fix (RF) leg types is highly preferred. The lateral trajectory can then—based on these two segment types—be constructed using only straight legs and constant radius turns (see Figure 2, left sub-figure). Parameterization of the variables defining these segments (such as length, turn radius and heading change) permits a significant freedom in the optimization of the ground track with a minimum number of parameters required. It is noted that with a given turn radius R, and the local airspeed V known, the bank angle μ is no longer required as a control input to the model, as it can be determined from

$$\mu = \pm \tan^{-1}\left(\frac{V^2}{gR}\right) \tag{5}$$

Vertical path parameterization

The synthesis of the vertical profile is based on the premise that descending and/or decelerating is not allowed throughout a departure procedure. To parameterize the vertical profile, the trajectory is subdivided into a number of segments. In each segment, the two control inputs are kept constant. The control inputs for a segment are either directly prescribed based on operational requirements or designated as optimization parameters. It is readily clear that the number of segments within a procedure (and thus the number of control parameters) has a direct relation with the freedom to optimize the trajectory, but also with the computational effort required to obtain a converged solution.
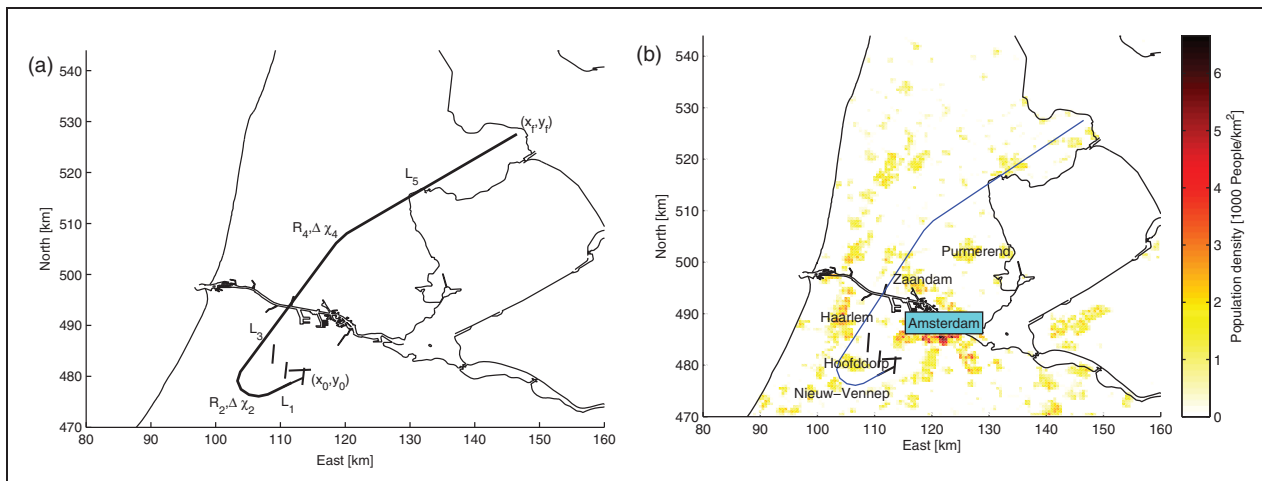

Figure 2. Ground track parameterization.

A switch from one segment to the next is triggered when a defined capture condition is met. Capture conditions may include reaching a specified target value of altitude, speed or along-track distance. Target values for the capture conditions are usually specified upfront, but are occasionally designated as optimization parameters.

A key feature of the proposed aircraft performance model is the introduction of normalized control (optimization) parameters in each segment. When considering the flight path angle γ in segment i, the normalized control optimization parameter $\gamma_{n,i}$ is defined as ($0 \leqslant \gamma_{n,i} \leqslant 1$)

$$\gamma_{n,i} = \frac{\gamma_i - \gamma_{\min,i}}{\gamma_{\max,i} - \gamma_{\min,i}} \qquad (6)$$

where the subscript n indicates a normalized control optimization parameter. The subscripts max,i and min,i denote, respectively, the maximum and minimum permissible value for segment i. It is important to emphasize that the value of $\gamma_{\max,i}$ needs to be determined for each time step in each segment separately. In contrast, the lower limit $\gamma_{\min,i}$ is generally set to $0°$ for all segments, as it basically results from the requirement that in a departure procedure descending is not permitted.

The normalized thrust setting $T_{n,i}$ ($0 \leqslant T_{n,i} \leqslant 1$) is defined in a similar fashion

$$T_{n,i} = \frac{T_i - T_{\min,i}}{T_{\max,i} - T_{\min,i}} \qquad (7)$$

The value of $T_{\max,i}$ is determined by the maximum available thrust setting, either $T_{T/O}$ (maximum take-off thrust) or T_{CL} (maximum climb thrust), depending on the flight stage. Finally, the value $T_{\min,i}$ is again determined separately for each time step in each flight segment and is subject to the requirement that it should never drop below the value to maintain steady level flight.

In flight segments where neither of the two normalized control parameters is a priori prescribed, the order in which the normalized control parameters are evaluated is of vital importance. The evaluation starts by assessing $T_{\min,i}$ in equation (7) under the assumption that $\gamma_i = \gamma_{min,i} = 0°$, while maintaining airspeed. From equation (1) it then follows that, in order to maintain airspeed, the thrust should equal the drag force, and hence $T_{\min,i} = D(h,V,\mu,W)$. Using the maximum available thrust $(T_{T/O}$ or $T_{CL})$, equation (1) subsequently yields the maximum allowed flight path angle $\gamma_{\max,i}$ in equation (6), again assuming that the aircraft maintains its airspeed (no deceleration allowed!).

The true benefit of the adopted parameterization is readily clear: any choice for the values of the two normalized control parameters $\gamma_{n,i}$, $T_{n,i}$ will always result in a feasible solution for the considered segment, without compromising the extent of the control parameter search space. When one of the normalized control parameters is *a priori* prescribed in a given segment (resulting from operational requirements), the remaining normalized control parameter is readily evaluated along the lines indicated above.

Coupling of vertical and horizontal profiles

Although the horizontal and vertical trajectory profiles are essentially generated independently, the coupling of the horizontal and vertical profiles cannot be completely ignored in the optimal trajectory synthesis process. The coupling of the vertical and horizontal profiles particularly manifests itself in the imposition of the terminal boundary conditions and in the enforcement of the bank angle constraint.

The aircraft is required to reach a terminal position (x_f, y_f) at a prescribed altitude and airspeed (see Figure 2, left sub-figure). Since decelerations and descents are not allowed during a departure, these altitude and airspeed terminal boundary conditions also represent the maximum altitude/speed values attained throughout the departure procedure. The potential problem of overshooting the airspeed or altitude terminal boundary conditions that may occur in the forward trajectory propagation process can be readily circumvented. If during any segment the final altitude is reached, first the maximum flight path angle is set to $0°$. Evaluation of equation (6) will then yield $\gamma_i = 0°$ regardless of the value of $\gamma_{n,i} \in [0,1]$ and the aircraft will remain at its altitude for the remainder of the segment. If subsequently in the process the maximum airspeed is also reached, accelerations are no longer allowed, and hence $T_{\max} = T_{\min} = D$ for any $T_{n,i} \in [0,1]$. In case the maximum airspeed is reached first, the same process is applied but in reversed order, i.e. determining the thrust setting first, and the resulting flight path angle next.

The problem of undershooting the airspeed or altitude boundary conditions at the end of the trajectory integration process is somewhat more difficult to handle. To deal with this particular problem, an additional final (N^{th}) segment has been added to the vertical profile in which both the normalized flight path angle and thrust setting are prescribed to be $\gamma_{n,N} = T_{n,N} = 1$. If at the start or during this segment either of the final boundary conditions is met, the same methodology applies as described above. The required length of this segment depends on the energy deficit between the start of the segment and the final conditions. An overestimation of this length could force the aircraft to climb and accelerate prematurely. However, in this study it was found that in all Pareto-optimal trajectories the aircraft had already reached its imposed final conditions well before reaching the final segment. In essence the adopted methodology ensures that, even though the

bounds of the normalized optimization parameters $[\gamma_{n,i}, T_{n,i}]$ are constant within a segment, the bounds of the actual controls $[\gamma_i, T_i]$ are continuously adapted according to the requirements of the local conditions.

The final issue to be dealt with relates to the imposition of bank angle limits. For the design of departure procedures ICAO defines a progressive maximum bank angle limit that is dependent on altitude $(\mu_{max} = \mu_{max}(h))$.[16] However, as outlined in Section Lateral track parameterization, the bank angle does not represent a separate optimization parameter in the present formulation, but is implicitly defined as a function of several other optimization parameters. Although in the evaluation of equation (5), the turn radius R is known before the integration of the horizontal path dynamics takes place, the local airspeed V is not. To deal with the coupling between the vertical and lateral profiles when imposing a bank angle limit, it was decided to directly include the bank angle constraint in the optimization formulation, by adding a penalty to the optimization objectives on any violation of the expression $\mu_{max} - |\mu| \geqslant 0$. It is noted that the bank angle constraints represent the only side constraints in the overall optimization formulation proposed herein.

Example scenario

To illustrate the capabilities of the optimization framework and the modeling and parameterization approach, one of the current standard instrument departures (SIDs) at AMS has been optimized for noise, fuel burn, and local NO_x emissions. The so-called Spijkerboor departure (see Figure 2, right sub-figure) starts from runway 24. It passes close by the communities of Hoofddorp and Haarlem, where most of the noise nuisance occurs. Trajectory optimization is commenced at screen height (50 ft) and at take-off safety speed $V_2 + 10$ kts with the landing gear retracted and departure flaps selected. The exit conditions are derived from the existing SID, namely an airspeed of 250 kts EAS and an altitude of 6000 ft. When the existing ground track is considered, it can be inferred that the ground track to be optimized can be segmented into five RNP legs, i.e. three straight (TF) legs and two constant radius (RF) turns. The optimization parameters that define the ground track structure are listed in Table 1, along with the

Table 1. Ground track parameters.

Parameter	Current SID	Lower bound	Upper bound
L_1	4100 m	614 m	10,000 m
R_2	3183 m	2000 m	10,000 m
$\Delta\chi_2$	152.4°	32°	170°
L_3	29,150 m	1000 m	50,000 m
R_4	7500 m	2000 m	10,000 m

SID: standard instrument departure.

parameters bounds used in this study, as well as the values for the current SID.

In order to parameterize the procedure, the vertical profile is subdivided into eleven segments. Furthermore, it is assumed that the procedure complies with the regulation applying to the ICAO-defined Noise Abatement Departure Procedures (NADP) 1 and 2.[16] These procedures prescribe full take-off thrust to be applied to at least 800 ft, whilst maintaining $V_2 + 10$ kts. Between 800 and 1500 ft altitude, the thrust is then reduced to maximum climb thrust; this cutback altitude is the first optimization parameter, h_1. Above the cutback altitude, the NADPs are then distinguished by a focus on either climbing or accelerating. The NADP-1 procedure continues climbing at $V_2 + 10$ knots until reaching an altitude of 3000 ft, and only then accelerates to V_{clean}, the airspeed where the flaps and slats are fully retracted. NADP-2 starts accelerating at a reduced flight path angle directly after thrust cutback, typically reaching V_{clean} already below 3000 ft altitude. Once the initial departure procedure is completed (i.e. upon reaching either 3000 ft altitude or V_{clean}), the aircraft is allowed a significantly deeper thrust cutback.[17]

To parameterize the initial part of the departure procedure, two segments are required. During the first segment the speed $V_2 + 10$ kts is maintained at maximum take-off thrust, which results in a prescribed flight path angle. Since both thrust and flight path angle are prescribed in the first segment, no optimization parameters are required for defining this segment. The ensuing segment is executed using maximum climb thrust, while the aircraft is allowed to either accelerate in level flight or to continue to climb at a flight path angle not exceeding the prevalent $\gamma_{max,2}$. These first two segments modeling the NADP have variable length, and are terminated once the capture conditions are reached (altitude or airspeed). The remaining nine segments of the departure procedure are evenly spaced over the remaining along track distance. Normalized flight path angle and thrust setting are used as optimization parameters in these segments. The resulting parameter bounds for the vertical procedure can be found in Table 2. It is noted that in this table also the parameter bounds are listed to fully comply with the existing ICAO-A departure procedure, which is essentially a variant of NADP-1. As the ICAO-A procedure was until recently the standard prescribed departure procedure at AMS, this procedure, along with the current ground track, has been used as the reference case to assess relative improvements in the optimized trajectories.

With 23 parameters describing the full 3D departure, the average runtime for each trajectory evaluation is 0.07 s or 1.0 s when noise impact is included, on a standard laptop CPU. All cases were run for 750 generations using a population size of 50. This results in good convergence of the optimization in 50 min to 6 h on dual CPU cores.

Table 2. Vertical profile parameters.

Parameter	ICAO-A reference	Lower bound	Upper bound
$T_{n,1}$	I	I	I
$T_{n,2}$	I	I	I
$T_{n,3-10}$	[0, I]	0	I
$T_{n,11}$	I	I	I
$\gamma_{n,1}$	I	I	I
$\gamma_{n,2}$	I	0	I
$\gamma_{n,3-10}$	[0,I]	0	I
$\gamma_{n,11}$	I	I	I
h_1	1500 ft	800 ft	1500 ft

Table 3. Results for the environmentally optimized example trajectories.

Case no.	Description	Time (s)	Fuel (kg)	NO$_x$ (g)	Awakenings
	Reference	609.9	572.5	2.07	5531
1	MF(−)	576.9	540.0	3.32	3396
2	MF(+)	649.3	590.8	3.39	3291
3	Fuel	528.4	507.3	3.18	5435
4	Noise	992.7	822.8	3.90	1375

Figure 3. Ground tracks for example trajectories.
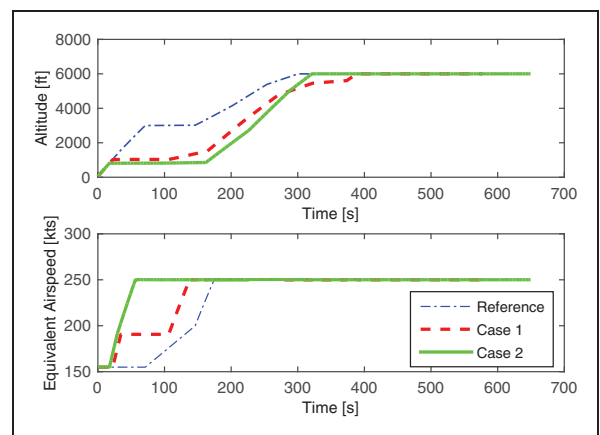
Figure 4. Airspeed and altitude profiles for the example trajectories.

Results

The numerical example presented concerns a Pareto-optimization of the Spijkerboor departure at AMS, using a Boeing 737-800 twin-engine aircraft model. Using GATAC, a bi-dimensional Pareto front has been generated, with fuel consumption and expected number of awakenings as the two criteria considered. The results, pertaining to four selected points on the Pareto front (i.e. cases 1–4), are summarized in Table 3. Although NO$_x$ has not been taken as an optimization criterion in this example, it has been included in Table 3 as a performance indicator for the four cases.

Cases 1 and 2 in Table 3 correspond to the available points on the Pareto front that are closest to the ICAO-A reference case in terms of the fuel burn (MF(−) differing −5.7% and MF (+) +3.2%, respectively). Cases 3 and 4 represent the two extreme cases, namely, the fuel-optimal solution and the noise-optimal solution.

Considering the very similar reduction in awakenings for cases 1 and 2 relative to the reference case (38.6% and 40.5%, respectively), it is interesting to inspect the ground tracks in Figure 3 and the airspeed and altitude profiles in Figure 4. It is clear that in both cases accelerating is preferred, in contrast to the ICAO-A reference case. More specifically, both solutions level 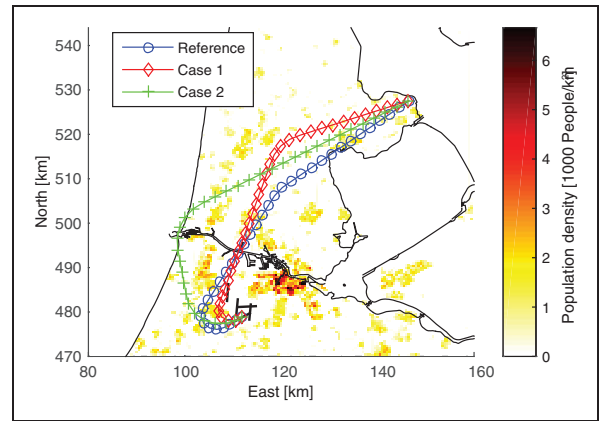off upon reaching 800 ft altitude and then accelerate. In case 1, acceleration is continued up to 190 kts—where the flaps are fully retracted—which is then maintained at a low thrust level to make a tight turn over Hoofddorp. In case 2, however, acceleration is continued until reaching 250 kts, while maintaining altitude. The higher speed does, however, require a larger turn radius, and hence the trajectory now circumnavigates the communities of Hoofddorp, Heemstede and Haarlem. This does, however, allow the aircraft to continue its climb over a less densely populated area close to the North Sea, and hence leads to a significant decrease in the number of awakenings. The cases 3 and 4 illustrate that potentially significant gains are attainable of over 10% for fuel, and over 75% in the number of awakenings, relative to the reference case.

Conclusions

A method is proposed to parameterize departure trajectories to avoid infeasibilities and constraints in environmental trajectory optimization using a genetic algorithm. The approach leads to a significant reduction in the number of required model evaluations, and hence in the required runtime.

An example scenario is presented optimizing an existing SID for fuel burn, and community noise impact. In contrast to the reference ICAO-A procedure, the Pareto-optimal solutions presented show a clear preference towards accelerating during the initial departure procedure, allowing the aircraft to retract its flaps and slats. This reduces the drag and as a result the fuel burn, and also has a positive effect on the noise impact as the increased airspeed reduces the exposure time.

For future research it is proposed to extent the scope of the proposed parameterization technique to different flight phases, notably to arrival procedures and routings.

Acknowledgement

Declaration of Conflicting Interests

Funding

References

1. Visser HG, Hebly SJ and Wijnen RAA. *Management of the environmental impact of airport operations*. New York: Nova Science Publishers, 2009.
2. Prats X, Puig V, Quevedo J, et al. Multi-objective optimisation for aircraft departure trajectories minimising noise annoyance. *Transport Res Part C* 2010; 18: 975–989.
3. Hartjes S, Visser HG and Hebly S. Optimisation of RNAV noise and emission abatement standard instrument departures. *Aeronaut J* 2010; 114: 757–767.
4. Hogenhuis RH, Heblij SJ and Visser HG. Optimization of RNAV noise abatement approach trajectories. *Proc IMechE, Part G: J Aerospace Engineering* 2011; 225: 513–521.
5. Fernandes de Oliveira R and Büskens C. Benefits of optimal flight planning on noise and emissions abatement at the Frankfurt airport. In: *Proceedings of AIAA guidance, navigation, and control conference*, Minneapolis, USA, 13–16 August 2012.
6. Richter M, Bittner M, Rieck M, et al. A non-cooperative bi-level optimal control problem formulation for noise minimal departure trajectories. In: *Proceedings of 29th international congress of the aeronautical sciences*, St. Petersburg, Russia, 7-12 September 2014.
7. Torres R, Bes C, Chaptal J, et al. Optimal, environmentally-friendly departure procedures for civil aircraft. *J Aircraft* 2011; 48: 11–21.
8. Cleansky. Systems for Green Operations (SGO) Integrated Technology Demonstrator at a glance, www.cleansky.eu/sites/default/files/documents/fact_sheet_sgo_march_2011.pdf (2011, accessed 14 August 2015).
9. Chircop K, Xuereb M, Zammit-Mangion D, et al. Generic framework for multi-parameter optimization of flight trajectories. In: *Proceedings of 27th international congress of the aeronautical sciences*, Nice, France, 19–24 September 2010.
10. Deb K, Pratap A, Agarwal S, et al. Fast and elitist multiobjective genetic algorithm: NSGAII. *IEEE Trans Evolut Comput* 2002; 6: 182–197.
11. Rogero JM. *A genetic algorithm based optimisation tool for preliminary design of gas turbine combustors*. PhD Thesis, Cranfield University, UK, 2002.
12. International Civil Aviation Organization. ICAO Engine Exhaust Emissions Databank, Engine Exhaust Database, https://easa.europa.eu/document-library/icao-aircraft-engine-emissions-databank#1 (2015, accessed 14 August 2015).
13. Baughcum SL, Tritz TG, Henderson SC, et al. *Scheduled civil aircraft emissions inventories for 1992: Database development and analysis, Appendix D: Boeing Method 2 fuel flow methodology description*. Report NASA CR 4700, 1996.
14. Boeker ER, Dinges E, He B, et. al. *Integrated noise model (INM) version 7.0 technical manual*. Report FAA-AEE-08-01, Federal Aviation Administration, Office of Environment and Energy, Washington DC, USA, 2007.
15. Federal Interagency Committee on Aviation Noise. Effects of aviation noise on awakenings from sleep, http://www.fican.org/pdf/Effects_AviationNoise_Sleep.pdf (1997, accessed 14 August 2015).
16. International Civil Aviation Organization. Procedures for air navigation services – Aircraft operations. Vol. I, Flight Procedures, ICAO document number 8168, 2006.
17. Federal Aviation Administration. *Noise abatement departure profiles*. FAA Advisory Circular 91-53a, 1993.

Appendix

Notation

C_{D_0}	zero lift drag parameter
D	drag force
g	acceleration due to gravity
h	altitude
EI	emission index
K	induced drag parameter
$\dot{m}_f$	fuel flow rate
m_{NO_x}	mass of emitted NO_x
R	turn radius
S	wing surface area
SEL	sound exposure level
t	time
T	thrust force
V	airspeed
V_{clean}	clean configuration safety speed
V_2	take-off safety speed

W	aircraft weight	γ	flight path angle
x, y	ground track coordinates	μ	bank angle
χ	heading angle	ρ	air density